# Reaction of Aqueous 2-(*N*-Methylamino)ethanol Solutions with Carbon Dioxide. Chemical Species and Their Conformations Studied by Vibrational Spectroscopy and ab Initio Theories

**Keiichi Ohno,* Yutaka Inoue, Hiroshi Yoshida, and Hiroatsu Matsuura**

*Department of Chemistry, Faculty of Science, Hiroshima University, Kagamiyama, Higashi-Hiroshima 739-8526, Japan*

*Received: December 30, 1998; In Final Form: March 17, 1999*

The reaction systems of aqueous 2-(*N*-methylamino)ethanol (MAE) solutions with dissolved $CO_2$ ($CO_2$−MAE−$H_2O$ system) and of liquid MAE with dissolved $CO_2$ ($CO_2$−MAE system) have been studied by vibrational spectroscopy and ab initio theories. The chemical species, molecular conformations, and intramolecular and intermolecular hydrogen bonding in these systems have been elucidated. The species produced in the $CO_2$−MAE−$H_2O$ system are the carbamate anion ($MAECO_2^-$), the protonated cation ($MAEH^+$), hydrogencarbonate ion ($HCO_3^-$), and carbonate ion ($CO_3^{2-}$), while the species produced in the $CO_2$−MAE system are $MAECO_2^-$ and $MAEH^+$. In the $CO_2$−MAE−$H_2O$ system, MAE (secondary amine) reacts with $CO_2$ to form $MAECO_2^-$ and $MAEH^+$, and $MAECO_2^-$ subsequently reacts with $H_2O$ and $CO_2$ to form $MAEH^+$ and $HCO_3^-$. This reaction mechanism is contrasted with the mechanism for 2-(*N*,*N*-dimethylamino)ethanol (DMAE, tertiary amine), which reacts with $CO_2$ and $H_2O$ to form directly $DMAEH^+$ and $HCO_3^-$. In the liquid state and in aqueous solution, $MAECO_2^-$ molecules assume predominantly the $S^-G^-g^+$ conformation with the formation of strong intramolecular 1,6-OH···$O^-$ hydrogen bonding, and $MAEH^+$ molecules assume predominantly the $TG^{\pm}t$ conformation with the formation of strong intramolecular 1,4-$NH^+$···O hydrogen bonding. MAE molecules in the condensed phases, on the other hand, assume several conformations such as $TG^-x$ ($x$ = t, $g^-$, and $g^+$), $TG^+g^-$, and $G^-G^-g^+$ as the result of the competition of intermolecular interactions such as OH···O or OH···N hydrogen bonding and intramolecular interactions such as the 1,4-OH···N hydrogen bonding. The interconversion, depending on pH or addition/removal of $CO_2$, of strong ionic hydrogen bonding such as $NH^+$···O, $NH^+$···$O^-$, and OH···$O^-$ and nonionic hydrogen bonding such as OH···N and OH···O is clearly one of the important structural features in the $CO_2$−amine−$H_2O$ system and probably in biomolecular systems, where intramolecular and/or intermolecular interactions between nitrogen and oxygen atoms are involved.

## Introduction

The recovery and removal of carbon dioxide from flue gases by using $CO_2$−amine−$H_2O$ systems have been of fundamental interest and industrial importance in the problem of preventing global warming.[1−8] To understand the reaction mechanism of these systems, the identification of the chemical species produced in the system and the determination of their molecular conformations are essential. A survey of the literature indicates, however, that only a few relevant spectroscopic investigations have been reported to date.[9,10−13]

In a previous infrared and Raman spectroscopic study of a system of $CO_2$, 2-(*N*,*N*-dimethylamino)ethanol (DMAE) as a tertiary amine, and $H_2O$, we have shown the formation of protonated DMAE ($DMAEH^+$), hydrogencarbonate ion ($HCO_3^-$), and carbonate ion ($CO_3^{2-}$).[9] This indicates that DMAE acts as a Lewis base:

$$\mathrm{DMAE} + \mathrm{CO_2} + \mathrm{H_2O} \rightarrow \mathrm{DMAEH^+} + \mathrm{HCO_3^-}$$

$DMAEH^+$ molecules in aqueous solution assume predominantly the gauche$^{\mp}$−gauche$^{\pm}$−trans ($G^{\mp}G^{\pm}t$) conformation around the $H^+N-C-C-OH$ bonds, which is stabilized by strong intramolecular 1,4-$NH^+$···O hydrogen bonding, while DMAE molecules assume several conformations stabilized through the competition of the relevant intermolecular interactions and intramolecular interactions such as 1,4-OH···N hydrogen bonding. These results indicate that in aqueous solution the structure of a $DMAEH^+$ molecule is rather tight, while that of a DMAE molecule is flexible. The NMR[2] and kinetic studies[3−6] of the $CO_2$−secondary amine−$H_2O$ systems have shown, on the other hand, that the secondary amine reacts with $CO_2$ to form the carbamate ion. The carbamate ions have been shown to play an important role in the circulatory system of blood by carrying $CO_2$ and in photosynthesis by activating ribulose-1,5-bisphosphate carboxylase/oxygenase.[14,15]

In the present work, we have studied by infrared and Raman spectroscopy and ab initio molecular orbital and density functional theories the chemical species produced and their molecular conformations in a $CO_2$−secondary amine−$H_2O$ system, where a reaction of aqueous 2-(*N*-methylamino)ethanol (MAE) solution with $CO_2$ takes place, and have discussed the reaction mechanism of the system. We have also examined the system of liquid MAE and $CO_2$. To elucidate the relevant intramolecular and intermolecular interactions that may be involved in these systems, we have studied the conformation

10.1021/jp984821q CCC: $18.00 
Published on Web 05/11/1999

of MAE molecules in an argon matrix and in the condensed phases such as the solid and liquid states and aqueous solution.

## Experimental Section

MAE was supplied by Tokyo Kasei Kogyo. The matrix-isolation infrared spectra of MAE were measured by depositing a premixed gas of Ar/MAE = 1000 onto a cesium iodide plate cooled to 11 K by an Iwatani CryoMini D105 refrigerator. The deposited sample was kept at different constant temperatures, ranging from 11 to 41 K, for 10 min for each time and was then cooled to 11 K to record the spectra. The spectra of MAE in the solid state were measured by the same method but depositing pure gas of MAE onto a cesium iodide plate. These infrared spectra were recorded on a JASCO FT/IR-350 Fourier transform spectrometer using a DTGS detector by co-addition of 100 scans at a resolution of 1 $cm^{-1}$. The infrared spectra of liquid MAE without $CO_2$ and saturated with $CO_2$ and of tetrahydrofuran solution of MAE were recorded on a Nicolet Impact 400 Fourier transform spectrometer using a DTGS detector by co-addition of 200 scans at a resolution of 1 $cm^{-1}$.

The Raman spectra of MAE were measured for the solid and liquid states and for aqueous solutions. The spectrum for the solid state was measured at 77 K on the sample contained in a sealed ampule placed on a copper block cooled with liquid nitrogen. The spectra of the liquids, without $CO_2$ and saturated with $CO_2$ under atmospheric pressure, and of 30% aqueous solutions, without $CO_2$, with $CO_2$ slightly absorbed, and saturated with $CO_2$ under atmospheric pressure, were measured at 298 K. Raman spectra were also measured on liquid MAE saturated with hydrogen chloride and on a hydrochloric acid solution of MAE. The Raman spectra were recorded on a JEOL JRS-400D spectrometer equipped with a Hamamatsu R469 photomultiplier or a JASCO NR-1800 spectrometer equipped with a CCD detector by using the 514.5 nm line of an NEC GLG 3200 or 2162 argon ion laser.

## Calculations

The ab initio calculations using the restricted Hartree−Fock method (HF) were performed on all of the 27 possible conformers of MAE, 9 conformers of *N*-(2-hydroxyethyl)-methylcarbamate anion ($MAECO_2^-$), and 14 conformers of (2-hydroxyethyl)methylammoniun cation ($MAEH^+$). The calculations using the second-order Møller−Plesset perturbation theory (MP2) and density functional theory of B3LYP were performed on several of more stable conformers of the above-mentioned chemical species and several important conformers of *N*-(2-hydroxyethyl)-*N*-methylcarbamic acid ($MAECO_2H$) and its zwitterion ($MAEH^+CO_2^-$). In these HF, MP2, and B3LYP calculations, the 6-31G** or 6-31G* basis set was used to obtain the energies, molecular geometries, and harmonic vibrational wavenumbers. The wavenumbers calculated by the HF/6-31G** and B3LYP/6-31G* methods were scaled by factors 0.91 and 0.98, respectively, for the vibrations above 700 $cm^{-1}$ and by factors 0.94 and 1.00, respectively, for the vibrations below 700 $cm^{-1}$.[16] The calculations were carried out with the GAUSSIAN 94 program[17] using the default parameters.

## Results and Discussion

The conformational stabilities of MAE, the carbamate anion $MAECO_2^-$, and the ammonium cation $MAEH^+$ expected in the $CO_2$−MAE−$H_2O$ system will be described on the basis of the results of ab initio calculations. The infrared and Raman spectra of MAE in an argon matrix and in the condensed phases will then be analyzed in light of the normal vibration calculations,

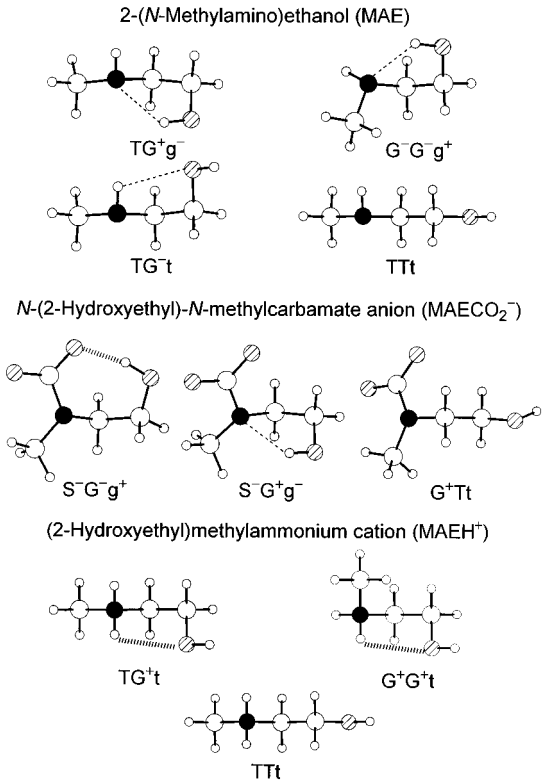


**Figure 1.** Molecular structures of the $TG^+g^-$, $G^-G^-g^+$, $TG^-t$, and TTt conformers of MAE (*S*-configuration), the $S^-G^-g^+$, $S^-G^+g^-$, and $G^+Tt$ conformers of $MAECO_2^-$ (*S*-configuration), and the $TG^+t$, $G^+G^+t$, and TTt conformers of $MAEH^+$. Black and hatched atoms indicate nitrogen and oxygen, respectively. A dashed line indicates intramolecular 1,4-OH···N or 1,4-NH···O hydrogen bonding, and stack bars indicate intramolecular 1,6-OH···$O^-$ hydrogen bonding ($MAECO_2^-$) or 1,4-$NH^+$···O hydrogen bonding ($MAEH^+$).

and the conformers present in the respective states and the effect of intramolecular and intermolecular interactions involved will be examined. Finally, the reaction mechanism of the $CO_2$−MAE and $CO_2$−MAE−$H_2O$ systems will be discussed on the basis of the infrared and Raman spectroscopic observations and the results of ab initio calculations.

**Conformational Stabilities of MAE, $MAECO_2^-$, and $MAEH^+$.** The relative energies of the conformers of MAE, $MAECO_2^-$, and $MAEH^+$ calculated by the HF/6-31G**, MP2/6-31G**, and B3LYP/6-31G** methods are given in Table 1, where the intramolecular interactions involved are indicated for the relevant conformers. One of the interesting interactions is intramolecular 1,5-CH···O interaction, which has been found to be important for the conformational stabilization of 1,2-dimethoxyethane[18−20] and 1-methoxy-2-(methylthio)ethane.[21] In Figure 1, the molecular structures of several typical conformers of MAE (*S*-configuration), $MAECO_2^-$ (*S*-configuration), and $MAEH^+$ are depicted. The conformations of MAE, $MAECO_2^-$, and $MAEH^+$ are designated by T or t for trans, G or g for gauche, and S for skew around the sequence of the $CH_3N$−C−C−OH bonds, where the lower-case letters apply to the conformation around the CC−OH bond. For MAE and $MAECO_2^-$, the conformations are shown only for the *S*-configuration throughout this paper, since the corresponding conformers of the *R*- and *S*-configurations are the enantiomers of each other, having the same energy and being spectroscopically equivalent; it may be remarked, however, that the alternation of the *R*- and *S*-configurations interchanges two gauche conformations, $G^+$ or $g^+$ and $G^-$ or $g^-$, and two skew conformations, $S^+$ and $S^-$.[22]

**TABLE 1: Relative Energies of Conformers of MAE, $MAECO_2^-$, and $MAEH^+$ Calculated by Various Methods**

| conformer | relative energy/kJ mol$^{-1}$ [a] HF/ 6-31G** | MP2/ 6-31G** | B3LYP/ 6-31G**[b] | interaction involved[c] |
|---|---|---|---|---|
| | MAE, $CH_3NH-CH_2-CH_2-OH$ | | | |
| $TG^+g^-$ | 0.0 | 0.0 | 0.0 (0.0) | OH···N |
| $G^-G^-g^+$ | 2.6 | 1.0 | 1.9 (2.0) | OH···N |
| $TG^-t$ | 5.1 | 8.3 | 8.3 (8.8) | NH···O |
| $TG^-g^-$ | 6.8 | 8.6 | 7.5 | NH···O |
| $TG^-g^+$ | 7.8 | 9.6 | 9.8 | |
| TTt | 11.1 | 18.0 | 16.8 (17.2) | |
| $TTg^-$ | 11.3 | 17.0 | 15.1 | |
| $G^+G^+t$ | 11.7 | 13.2 | 13.8 | NH···O |
| $TTg^+$ | 12.0 | 17.6 | 15.4 | |
| $G^+G^+g^+$ | 13.0 | | | NH···O |
| $G^-Tt$ | 14.5 | | | |
| $G^-Tg^+$ | 15.2 | | | |
| $G^-Tg^-$ | 15.6 | | | |
| $G^-G^+t$ | 16.6 | | | CH···O |
| $G^+G^+g^-$ | 16.8 | | | |
| $G^-G^+g^+$ | 17.6 | | | CH···O |
| $G^+Tt$ | 18.0 | | | |
| $G^+Tg^-$ | 18.1 | | | |
| $G^+Tg^+$ | 18.6 | | | |
| $G^+G^-t$ | 19.3 | | | CH···O |
| $G^+G^-g^-$ | 19.6 | | | CH···O |
| $TG^+t$ | 20.4 | | | |
| $G^-G^-t$ | 23.1 | | | |
| $G^+G^-g^+$ | 23.3 | | | |
| $TG^+g^+$ | ($TG^+g^-$) | | | |
| $G^-G^-g^-$ | ($G^-G^-g^+$) | | | |
| $G^-G^+g^-$ | ($TG^+g^-$) | | | |
| | $MAECO_2^-$, $CH_3N(CO_2^-)-CH_2-CH_2-OH$[d] | | | |
| $S^-G^-g^+$ | 0.0 | 0.0 | 0.0 | $OH\cdots O^-$ |
| $S^-G^+g^-$ | 20.0 | 20.3 | 28.6 | OH···N |
| $G^+Tg^-$ | 31.7 | 42.5 | 46.1 | |
| $G^+Tg^+$ | 39.1 | 49.5 | 51.9 | |
| $G^+Tt$ | 41.1 | 53.5 | ($G^+Tg^-$) | |
| $S^-G^-t$ | ($S^-G^-g^+$) | | | |
| $S^-G^-g^-$ | ($S^-G^-g^+$) | | | |
| $S^-G^+t$ | ($S^-G^+g^-$) | | | CH···O |
| $S^-G^+g^+$ | ($S^-G^+g^-$) | | | CH···O |
| | $MAEH^+$, $CH_3NH_2^+-CH_2-CH_2-OH$ | | | |
| $TG^\pm t$ | 0.0 | 0.0 | 0.0 | $NH^+\cdots O$ |
| $G^\pm G^\pm t$ | 3.2 | 1.3 | 2.8 | $NH^+\cdots O$ |
| TTt | 33.6 | 38.6 | 35.6 | |
| $G^\pm Tt$ | 38.6 | 42.1 | 39.7 | |
| $TG^\pm g^\pm$ | ($TG^\pm t$) | | | $NH^+\cdots O$ |
| $TG^\pm g^\mp$ | ($TG^\pm t$) | | | |
| $G^\pm G^\pm g^\pm$ | ($G^\pm G^\pm t$) | | | $NH^+\cdots O$ |
| $G^\pm G^\pm g^\mp$ | ($G^\pm G^\pm t$) | | | |
| $TTg^\pm$ | (TTt) | | | |
| $G^\pm Tg^\pm$ | ($G^\pm Tt$) | | | |
| $G^\pm Tg^\mp$ | ($G^\pm Tt$) | | | |
| $G^\pm G^\mp t$ | ($TG^\mp t$) | | | CH···O |
| $G^\pm G^\mp g^\pm$ | ($TG^\mp t$) | | | |
| $G^\pm G^\mp g^\mp$ | ($TG^\mp t$) | | | CH···O |

[a] In the case where the structure optimization failed, the conformation eventually obtained is given in parentheses. [b] The relative energies calculated by the B3LYP/6-31G* method are given in parentheses. [c] OH···N, intramolecular 1,4-OH···N hydrogen bonding; NH···O, intramolecular 1,4-NH···O hydrogen bonding; CH···O, intramolecular 1,5-CH···O interaction; $OH\cdots O^-$, intramolecular 1,6-OH···$O^-$ hydrogen bonding; $NH^+\cdots O$, intramolecular 1,4-$NH^+$···O hydrogen bonding. [d] The $S^-$ and $G^+$ conformations around the $CH_3N-CC$ bond are approximately −120° and 85°, respectively.

The ab initio calculations showed that the most stable conformer of MAE is $TG^+g^-$ and the second most stable conformer is $G^-G^-g^+$. The stable conformers following these are $TG^-t$, $TG^-g^-$, and $TG^-g^+$. It may be noted that the above-mentioned conformers are more stable than the TTt conformer with the least steric repulsion. The $TG^+g^-$ and $G^-G^-g^+$ conformers are stabilized by intramolecular 1,4-OH···N hydrogen bonding as justified by the calculated results for the nonbonded OH···N distance, 2.33−2.35 Å by HF/6-31G**, 2.15−2.18 Å by MP2/6-31G**, or 2.19−2.21 Å by B3LYP/6-31G**, which is considerably shorter than the sum of the van der Waals radii of hydrogen and nitrogen, 2.70 Å, and for the partial charges of atoms $O^{-0.65}-H^{+0.35}\cdots N^{-0.66}$ in units of *e* (elementary charge) by HF/6-31G**. The $TG^-t$ and $TG^-g^-$ conformers, on the other hand, are stabilized by intramolecular 1,4-NH···O hydrogen bonding; the calculated nonbonded NH···O distance is 2.44 Å (HF/6-31G**), 2.37−2.40 Å (MP2/6-31G**), or 2.41−2.43 Å (B3LYP/6-31G**), in comparison with the sum of the van der Waals radii of hydrogen and oxygen, 2.60 Å, and the partial charges of atoms are $N^{-0.64}-H^{+0.29}\cdots O^{-0.65}$ (HF/6-31G**). The above results of the conformational stabilities show that intramolecular 1,4-OH···N hydrogen bonding is stronger than intramolecular 1,4-NH···O hydrogen bonding, in good agreement with the experimental results for 2-aminoethanol.[23] For MAE, the least stable conformers are $TG^+t$, $G^-G^-t$, and $G^+G^-g^+$ with N···O or $CH_3\cdots HO$ repulsions.

For $MAECO_2^-$, the out-of-plane angle determined by the three bonds around the nitrogen atom was calculated to be less than 20°, indicating that the three bonds are almost coplanar. The most stable conformer is $S^-G^-g^+$, which is far more stable than others. The high stability of this conformer is explained by strong intramolecular 1,6-OH···$O^-$ hydrogen bonding, as supported by the calculated nonbonded $OH\cdots O^-$ distance, 1.74 Å (HF/6-31G**), 1.62 Å (MP2/6-31G**), or 1.60 Å (B3LYP/6-31G**), which is much shorter than the sum of the van der Waals radii of hydrogen and oxygen, 2.60 Å, and by the calculated partial charges $O^{-0.72}-H^{+0.40}\cdots O^{-0.80}$ (HF/6-31G**).

For $MAEH^+$, the $TG^\pm t$ and $G^\pm G^\pm t$ conformers are exceedingly more stable than others, as stabilized by strong intramolecular 1,4-$NH^+$···O hydrogen bonding; the calculated nonbonded $NH^+\cdots O$ distance is 2.12−2.13 Å (HF/6-31G**), 2.01−2.02 Å (MP2/6-31G**), or 1.98−2.01 Å (B3LYP/6-31G**), which is significantly shorter than the sum of the van der Waals radii of hydrogen and oxygen, 2.60 Å, and the calculated partial charges are $N^{-0.61}-H^{+0.41}\cdots O^{-0.66}$ (HF/6-31G**).

The relative stabilities calculated by the HF/6-31G** method for the TT*x* conformers (*x* = t, $g^+$, and $g^-$) of MAE and for the $G^+Tg^-$ conformer of $MAECO_2^-$ are considerably different from those calculated by the MP2/6-31G** and B3LYP/6-31G** methods. These consequences indicate that the effects of intramolecular 1,4-OH···N and 1,6-OH···$O^-$ hydrogen bonding are evaluated to be more significant in the MP2/6-31G** and B3LYP/6-31G** calculations than in the HF/6-31G** calculations.

**Matrix-Isolation Infrared Spectra of MAE.** Figure 2 shows the infrared spectra of MAE in an argon matrix with Ar/MAE = 1000 and the spectra calculated by the B3LYP/6-31G* method for the $TG^+g^-$, $G^-G^-g^+$, $TG^-t$, and TTt conformers of MAE. The infrared spectra in the 2500−3700 $cm^{-1}$ region are shown in Figure 3, where the spectra in other phases are also shown. The observed wavenumbers for an argon matrix and other phases and the calculated wavenumbers are given in Table 2. The observation of bands at 540 and 545 $cm^{-1}$ indicates that the $TG^+g^-$, $G^-G^-g^+$, and/or $TG^-t$ conformer is present in an argon matrix, because the HF/6-31G** calculations and the B3LYP/6-31G* calculations (wavenumbers shown in parentheses) predict the skeletal deformation vibration for $TG^+g^-$ at 550 (543) $cm^{-1}$, for $G^-G^-g^+$ at 546 (546) $cm^{-1}$, and for $TG^-t$ at 536 (534) $cm^{-1}$, while for TTT the calculations predict the

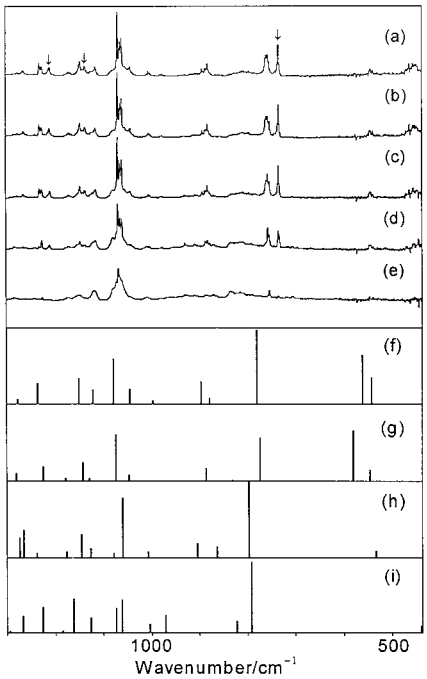


**Figure 2.** Infrared spectra of MAE in an argon matrix measured (a) immediately after the sample deposition at 11 K and (b, c, d, e) after annealing at 26, 32, 38, and 41 K, respectively, and the spectra calculated by the B3LYP/6-31G* method for (f) $TG^+g^-$, (g) $G^-G^-g^+$, (h) $TG^-t$, and (i) TTt conformers of MAE. The bands, which decrease in relative intensity on annealing, are marked with an arrow in (a).

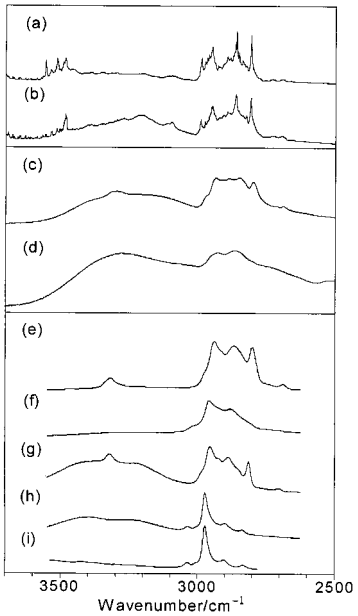


**Figure 3.** Infrared spectra of MAE in (a) argon matrix immediately after the sample deposition at 11 K, (b) argon matrix after annealing at 41 K, (c) the liquid state at 298 K, and (d) the liquid state saturated with $CO_2$ at 298 K, and Raman spectra at 298 K of MAE in (e) the liquid state, (f) the liquid state saturated with $CO_2$, (g) 30% aqueous solution, (h) 30% aqueous solution saturated with $CO_2$, and (i) hydrochloric acid solution.

highest-wavenumber skeletal deformation vibration at 448 (442) cm$^{-1}$. The present experimental results are consistent with the calculated results of the conformational stabilities given in Table 1 that the $TG^+g^-$, $G^-G^-g^+$, and $TG^-t$ conformers are the most stable conformers of MAE.

The conformational equilibration of MAE molecules in the matrix was monitored by annealing the sample, since the annealing process induces a transformation of less stable conformations into the most stable conformation.[24,25] When the matrix-isolation spectra on annealing is analyzed, however, the effects of molecular aggregation and multiple sites should also be taken into account, since these effects often cause spectral changes and band splittings. In Figure 2, many bands show splittings of 3−8 cm$^{-1}$, which can be interpreted to be associated with the existence of different conformers, the existence of monomer and dimer, or the existence of different trapping sites. When annealed at 38 K, each one of the split bands in pairs, such as the ones at 447, 732, 756, 815, 835, 878, and 1003 cm$^{-1}$, increases in intensity, while the splitting of the bands persists. The bands mentioned above are therefore most probably assigned to the dimer species of MAE. The annealing at 38−40 K increases the intensities of the weak bands at 831, 930, and 1079 cm$^{-1}$. These bands are ascribable to the aggregated species of the $TG^-x$ conformers ($x$ = t, $g^+$, and $g^-$) that are stabilized by intermolecular hydrogen bonding, being consistent with the observation of a band at 3220 cm$^{-1}$ (Figure 3) assigned to the intermolecular hydrogen-bonded O−H stretching vibration.

In the 700−800 cm$^{-1}$ region, two medium-intensity bands with small splittings are observed at about 735 and 760 cm$^{-1}$, and the former becomes weaker relative to the latter on annealing at 38−40 K (Figure 2). The HF/6-31G** calculations and the B3LYP/6-31G* calculations (wavenumbers shown in parentheses) predict the NH deformation vibration with strong infrared intensity at 773 (781) cm$^{-1}$ for $TG^+g^-$, 769 (774) cm$^{-1}$ for $G^-G^-g^+$, and 789 (798) cm$^{-1}$ for $TG^-t$. These results show that the bands at 735 and 760 cm$^{-1}$ are assigned to the $G^-G^-g^+$ and $TG^+g^-$ conformers, respectively, while the weak band at 831 cm$^{-1}$ is assigned to the $TG^-t$ conformer.

The intensities of the bands at 1137 and 1210 cm$^{-1}$, as marked with an arrow in Figure 2a, decrease on annealing with respect to the bands at 1147 and 1226 cm$^{-1}$, respectively. The HF/6-31G** and B3LYP/6-31G* calculations give the wavenumber of the vibration associated with the C−N stretching and $CH_3$ rocking modes at 1159 (1151) cm$^{-1}$ for $TG^+g^-$ and 1153 (1142) cm$^{-1}$ for $G^-G^-g^+$, and the wavenumber of the $CH_2$ twisting vibration at 1238 (1237) cm$^{-1}$ for $TG^+g^-$ and 1221 (1225) cm$^{-1}$ for $G^-G^-g^+$. These results indicate that the bands at 1137 and 1210 cm$^{-1}$ are due to the $G^-G^-g^+$ conformer and the bands at 1147 and 1226 cm$^{-1}$ are due to the $TG^+g^-$ conformer.

The existence of the $TG^+g^-$ and $G^-G^-g^+$ conformers in the matrix, but not of the $TG^-t$ and TTt conformers, is confirmed by examining the O−H stretching region of the spectra (Figure 3a,b). The O−H stretching bands are observed at 3485, 3516, and 3555 cm$^{-1}$ at 20 K and at 3485 cm$^{-1}$ at 41 K. These bands are assigned to the hydrogen-bonded O−H stretching vibrations of monomer with intramolecular O−H···N hydrogen bonding or dimer.[26−28] In the spectrum at 41 K, a broad band is observed at 3220 cm$^{-1}$, assignable to intermolecular hydrogen-bonded O−H stretching vibrations. The O−H stretching wavenumbers calculated by the B3LYP/6-31G* method are 3565, 3550, 3689, and 3686 cm$^{-1}$ for the $TG^+g^-$, $G^-G^-g^+$, $TG^-t$, and TTt conformers, respectively.

On the basis of the above spectral elucidation, we conclude that molecules of MAE assume the $TG^+g^-$ and $G^-G^-g^+$ conformers in the matrix, the former being more stable than the latter.

**Infrared and Raman Spectra of MAE in the Condensed Phases.** The infrared and Raman spectra of MAE in the liquid

**TABLE 2: Observed and Calculated Vibrational Wavenumbers[a] ($cm^{-1}$) of MAE**

| infrared[b] | | | Raman[b] | | | HF/6-31G**[d,e] | | | B3LYP/6-31G*[d,f] | | |
|---|---|---|---|---|---|---|---|---|---|---|---|
| matrix (11 K) | matrix (38 K) | liquid (298 K) | solid (77 K) | liquid (298 K) | aq soln[c] (298 K) | $TG^+g^-$ | $G^-G^-g^+$ | $TG^-t$ | $TG^+g^-$ | $G^-G^-g^+$ | $TG^-t$ |
| 1171 vw | 1171 vw | | 1170 w | 1169 w | 1171 w | 1172 (6, 4) | 1180 (11, 0.7) | 1184 (13, 1) | 1177 (4) | 1179 (4) | 1177 (7) |
| 1166 vw | | 1166 w | 1159 w | | | | | | | | |
| 1147 w | 1147 w | 1145 m | 1151 w | 1143 mw | 1147 w | 1159 (33, 3) | | | 1151 (34) | | |
| 1137 w | 1136 vw | | | | | | 1153 (32, 4) | 1145 (32, 9) | | 1142 (34) | 1146 (30) |
| 1124 vw | | | | | | | 1132 (12, 4) | | | 1130 (4) | |
| 1116 w | 1116 w | 1116 s | 1123 m | 1115 m | 1113 ms | 1128 (29, 9) | | 1123 (22, 5) | 1123 (19) | | 1128 (12) |
| | 1079 w | | 1080 m | | | | | 1084 (86, 4) | | | 1079 (5) |
| | 1072 w | | | | | | | | | | |
| 1069 s | 1069 s | | | | | 1099 (108, 4) | | | 1080 (86) | | |
| 1064 m | 1064 m | | | | | | 1092 (113, 5) | | | 1075 (89) | |
| 1061 m | 1061 m | 1060 vvs | 1069 s | 1061 s | 1052 s | | | 1052 (8, 2) | | | 1060 (77) |
| 1054 vw | | | | | | | 1045 (19, 1) | | | 1047 (10) | |
| 1043 w | 1044 vw | 1029 m | | 1026 m | 1022 s | 1080 (7, 3) | | | 1045 (20) | | |
| 1006 w | 1008 vw | 1008 w | 1009 m | 1011 mw | 1012 sh, m | 997 (7, 4) | | 1000 (10, 3) | 997 (5) | | 1008 (8) |
| | 1003 vw | | | 989 w | 990 w | | | | | | |
| 977 vw | 978 vw | 962 sh, vw | | 973 vw | 971 vw | | 975 (0.8, 7) | | | 981 (0.4) | |
| | 930 vw | | 951 s | | | | | 898 (20, 5) | | | 905 (19) |
| 909 vw | 909 vw | | | 909 sh, w | | | | | | | |
| 893 w | | 898 br, m | | 895 m | 894 br, m | 892 (21, 3) | | | 896 (29) | | |
| 887 w | 887 w | | | | | | 883 (22, 7) | | | 887 (23) | |
| 882 w | 882 w | | 881 m | 881 sh, w | | 859 (6, 9) | | 856 (7, 6) | 879 (7) | | 864 (14) |
| | 878 vw | | 870 w | | | | | | | | |
| | 870 vw | 869 m | | | | | 821 (8, 10) | | | 832 (1) | |
| | 835 w | | 843 vs | 847 sh, vw | | | | | | | |
| 827 vw | 831 w | 826 ms | 838 s | 830 ms | 831 s | | | 789 (116, 7) | | | 798 (99) |
| 808 vw | 815 w | | | | | | | | | | |
| 801 vw | 808 w | 800 sh, m | | | | | | | | | |
| 796 vw | 791 vw | | | | | | | | | | |
| 760 m | 756 m | 775 sh, m | | | | 773 (114, 6) | | | 781 (97) | | |
| 756 m | 754 w | | | | | | | | | | |
| 735 m | 735 m | | | | | | 769 (94, 3) | | | 774 (82) | |
| | 732 w | | | | | | | | | | |
| 545 w | 546 w | | 551 m | | | 550 (10, 2) | | | 543 (35) | | |
| 540 w | 540 vw | 539 w | 543 m | 538 m | 537 m | | 546 (32, 0.5) | 536 (10, 1) | | 546 (21) | 534 (9) |
| | | | | 504 w | 512 w | | | | | | |
| 465 w | | | | | | | | | | | |
| 458 w | 455 w | 458 vw | | 452 vw | 457 vw | 469 (130, 2) | 473 (121, 2) | | 562 (64) | 580 (97) | |
| 451 w | 447 w | | | | | | | | | | |
| | | | | 423 m | 422 m | | 414 (4, 0.3) | | | 413 (3) | |
| | | | 389 m | | | | | | | | |
| | | | 363 m | 369 m | 371 m | 368 (3, 1) | | 364 (2, 0.8) | 369 (3) | | 366 (2) |
| | | | 311 m | | | | 299 (3, 0.4) | 294 (20, 1) | | 305 (3) | 295 (17) |
| | | | 293 vw | 291 w | 284 br, vw | 268 (0.4, 0.0) | | 259 (94, 2) | 268 (0.1) | | 261 (39) |
| | | | 282 vw | | | 250 (3, 0.2) | 233 (1, 0.1) | 238 (35, 0.6) | 259 (3) | 220 (2) | 240 (69) |
| | | | 174 w | | | 163 (4, 0.1) | 163 (2, 0.1) | 157 (1, 0.1) | 167 (4) | 163 (3) | 160 (0.6) |
| | | | 145 w | | | | | | | | |
| | | | 133 w | | | | | | | | |
| | | | 108 w | | | 105 (0.5, 0.2) | 87 (2, 0.2) | 111 (7, 0.1) | 109 (1) | 95 (2) | 113 (7) |
| | | | 97 w | | | | | | | | |
| | | | 67 vs | | | | | | | | |

[a] Wavenumbers above 1200 $cm^{-1}$ are not included in this table because they are insensitive to the conformation. [b] Approximate relative intensities: vvs, very very strong; vs, very strong; s, strong; ms, medium strong; m, medium; mw, medium weak; w, weak; vw, very weak; sh, shoulder; br, broad. [c] 30% aqueous solution without $CO_2$. [d] For scale factors, see text. [e] Infrared intensities in km $mol^{-1}$ and Raman intensities in $Å^4$ $amu^{-1}$ are given in parentheses in this order. [f] Infrared intensities in km $mol^{-1}$ are given in parentheses.

and solid states and in aqueous solution are shown in Figure 4, where the calculated Raman spectra of six stable conformers of MAE, $TG^+g^-$, $G^-G^-g^+$, $TG^-t$, $TG^-g^-$, $TG^-g^+$, and TTt, are also shown. The infrared spectra in the 700−900 $cm^{-1}$ region of MAE in tetrahydrofuran solutions and in the supercooled liquid and solid states are shown in Figure 5. A comparison with the matrix-isolation infrared spectra indicates that the bands at 735 and 760 $cm^{-1}$ in the matrix are missing in the Raman and infrared spectra in the solid state. Figure 4 shows that the solid-state spectrum matches more closely the calculated spectra of the $TG^-x$ conformers ($x$ = t, $g^-$, and $g^+$) than those of others. Considering the results that the calculated spectra of $TG^-t$, $TG^-g^-$, and $TG^-g^+$ are similar to one another and that the CC−OH bond in 1-butanol assumes both trans and gauche conformations in the solid state,[26] we conclude that the conformers of MAE in the solid state are $TG^-x$. Most of the Raman bands observed in the liquid state and in aqueous solution correspond to the bands in the solid state. The Raman spectra in the liquid state and in aqueous solution show, however, a number of additional bands such as those at 423, 452, 895, 973, and 1026 $cm^{-1}$. These bands are assigned, on the basis of the calculated results, to the $TG^+g^-$ or $G^-G^-g^+$ conformer (Table 2).

Figure 5 shows that the spectral features in the 700−900 $cm^{-1}$ region change drastically depending on the phase. The dilute tetrahydrofuran solution exhibits a shoulder band at 744 $cm^{-1}$,

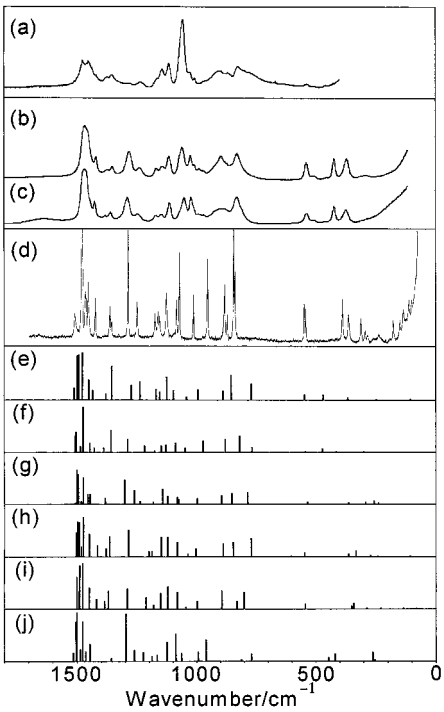


**Figure 4.** (a) Infrared spectrum of MAE in the liquid state at 298 K, (b) Raman spectrum of MAE in the liquid state at 298 K, (c) Raman spectrum of 30% aqueous solution of MAE at 298 K, (d) Raman spectrum of MAE in the solid state at 77 K, and the Raman spectra calculated by the HF/6-31G** method for (e) $TG^+g^-$, (f) $G^-G^-g^+$, (g) $TG^-t$, (h) $TG^-g^-$, (i) $TG^-g^+$, and (j) TTt conformers of MAE.

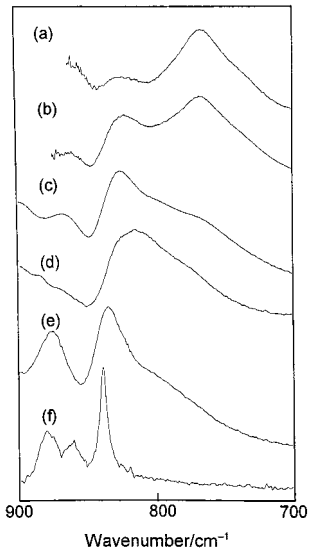


**Figure 5.** Infrared spectra of MAE in (a) 5% and (b) 17% tetrahydrofuran solutions at 298 K (the bands of tetrahydrofuran have been subtracted from the original spectra), (c) the liquid state at 298 K, (d) the supercooled liquid state immediately after the deposition of vapor MAE at 11 K, (e) the supercooled liquid state after annealing at 160 K, and (f) the solid state after annealing at 200 K.

a strong band at 766 cm$^{-1}$, and a weak band at 822 cm$^{-1}$ (Figure 5a), which are assigned to the $G^-G^-g^+$, $TG^+g^-$, and $TG^-x$ conformers, respectively (Table 2). With increasing concentration, the intensities of the first two bands decrease, while the intensity of the last band increases (Figure 5a−c). The spectrum in the supercooled liquid state exhibits a shoulder band at 785 cm$^{-1}$ and a broad band at 814 cm$^{-1}$ (Figure 5d). On solidification, the former band disappears and the latter band shifts to 839 cm$^{-1}$ (Figure 5f). These spectral features are consistent with

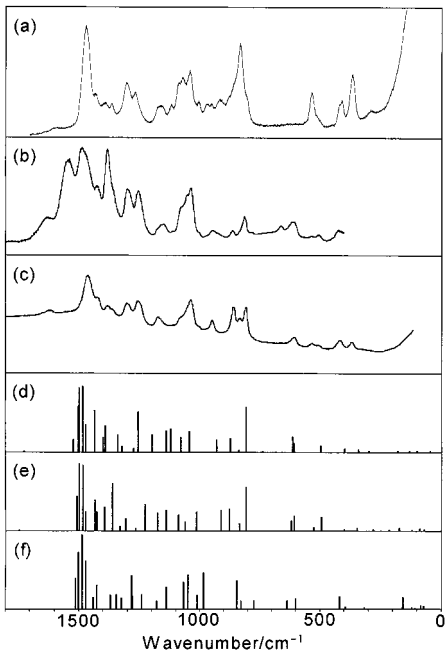


**Figure 6.** (a) Raman spectrum at 298 K of MAE in the liquid state saturated with hydrogen chloride, (b) infrared spectrum at 298 K of MAE in the liquid state saturated with $CO_2$, (c) Raman spectrum at 298 K of MAE in the liquid state saturated with $CO_2$, and the Raman spectra calculated by the HF/6-31G** method for (d) $S^-G^-g^+$, (e) $S^-G^+g^-$, and (f) $G^+Tt$ conformers of $MAECO_2^-$.

the interpretation of the infrared spectra in the matrix and the Raman spectra in the liquid and solid states.

The above results for MAE show that the $TG^-x$ conformers ($x$ = t, $g^-$, and $g^+$) are dominant in the condensed phases, although the $TG^+g^-$ and/or $G^-G^-g^+$ conformer is also present in the liquid state and in aqueous solution. Since intermolecular interactions such as OH···O and OH···N hydrogen bonding should be more important than intramolecular interactions in the condensed phases, the $TG^-x$ conformers are stabilized most probably by the relevant intermolecular interactions. The $TG^+g^-$ and $G^-G^-g^+$ conformers, on the other hand, are stabilized by intramolecular 1,4-OH···N hydrogen bonding.

**$CO_2$−MAE System.** When $CO_2$ is absorbed in liquid MAE, the liquid becomes viscous. The following exothermic reaction is very likely to occur in this system:[1,3,4,29,30]

$$2CH_3NHCH_2CH_2OH\ (MAE) + CO_2 \rightleftharpoons CH_3N(CO_2^-)CH_2CH_2OH\ (MAECO_2^-) + CH_3NH_2^+CH_2CH_2OH\ (MAEH^+) \quad (1)$$

The formation of the carbamic acid ($MAECO_2H$)[31,32] or its zwitterion ($MAEH^+CO_2^-$)[1,3,4] would also be expected:

$$CH_3NHCH_2CH_2OH\ (MAE) + CO_2 \rightarrow CH_3N(CO_2H)CH_2CH_2OH\ (MAECO_2H) \quad (2)$$

$$CH_3NHCH_2CH_2OH\ (MAE) + CO_2 \rightarrow CH_3NH^+(CO_2^-)CH_2CH_2OH\ (MAEH^+CO_2^-) \quad (3)$$

We will discuss the reaction mechanism of the $CO_2$−MAE system on the basis of the analysis of infrared and Raman spectra and the results of ab initio calculations. The observed spectra of liquid MAE saturated with $CO_2$, along with other related spectra, are shown in Figures 3−7, and the calculated Raman spectra for several important conformers of $MAECO_2^-$ and

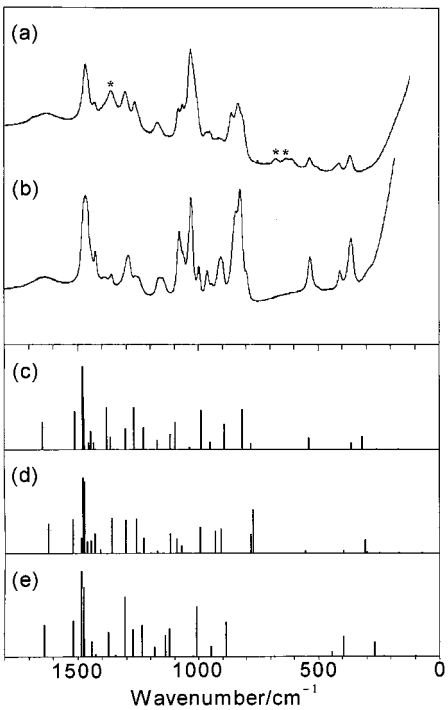


**Figure 7.** Raman spectra at 298 K of MAE in (a) 30% aqueous solution saturated with $CO_2$ and (b) hydrochloric acid solution, and the Raman spectra calculated by the HF/6-31G** method for (c) $TG^{\pm}t$, (d) $G^{\pm}G^{\pm}t$, and (e) TTt conformers of $MAEH^+$. The bands due to hydrogencarbonate ion are marked with an asterisk in (a).

$MAEH^+$ are shown in Figures 6 and 7. The observed wavenumbers for the infrared and Raman spectra and the calculated wavenumbers for the selected conformers of $MAECO_2^-$ and $MAEH^+$ are given in Table 3.

The infrared spectrum of liquid MAE saturated with $CO_2$ shows a very strong band at 1550 $cm^{-1}$ (Figure 6b). This band is assigned to the C═O stretching vibration of carboxylate, in agreement with the accepted region, 1550−1610 $cm^{-1}$, of this vibration for the $CO_2^-$ group.[33] Ammonium carbamate $NH_2$-$CO_2^-NH_4^+$ in fact gives a very strong infrared band at 1545 $cm^{-1}$ due to this vibration.[13] The infrared and Raman spectra of liquid MAE saturated with $CO_2$ show the bands associated with the $CO_2^-$ group at 610 and 606 $cm^{-1}$, respectively (Figure 6b,c). The present normal vibration calculations have interpreted these bands to be due to the deformation vibration of the $(N)CO_2^-$ group. These spectral findings for liquid MAE saturated with $CO_2^-$ prove that a chemical species $MAECO_2^-$ is formed in this liquid phase.

Other important spectral features of liquid MAE saturated with $CO_2$ are that the band of MAE at 3320 $cm^{-1}$ due to the N−H stretching vibration disappears on $CO_2$ absorption and that the band at 2801 $cm^{-1}$ due to the $(N)CH_3$ symmetric stretching vibration[10] shifts up to 2890 $cm^{-1}$ (Figure 3c−f). In lower-wavenumber regions, several bands such as those at 533 and 835 $cm^{-1}$ for liquid MAE saturated with $CO_2$ coincide with the corresponding bands for liquid MAE protonated by absorbing hydrogen chloride (Figure 6a,c). These observations suggest that part of MAE molecules are protonated as $MAEH^+$. The spectral analysis described above for liquid MAE saturated with $CO_2$ provides us with the evidence that the chemical species $MAECO_2^-$ and $MAEH^+$ are produced through reaction 1 by absorption of $CO_2$ in MAE.

We next consider a possibility of the formation of the carbamic acid ($MAECO_2H$) through reaction 2. The most clear evidence for carboxyl acid is a C═O stretching band of the carboxyl group in the 1650−1740 $cm^{-1}$ region.[33] In the infrared spectrum of liquid MAE saturated with $CO_2$, a very strong C═O stretching band is observed at 1550 $cm^{-1}$ as mentioned before, which is ascribed to carboxylate, but no band is observed in the region expected for carboxyl acid. This result of spectral analysis in the C═O stretching region indicates that $MAECO_2H$ is only an intermediate species, even if it is formed through reaction 2, and may react immediately with MAE to form $MAECO_2^-$ and $MAEH^+$. Carbamic acids (RR′NCOOH) have, in fact, not been isolated so far.[31,32] It may be remarked here, however, that the present calculations optimized the $S^-G^-g^+$ conformer of $MAECO_2H$ when the initial geometry was transferred from $MAECO_2^-$.

We should also consider a possibility of the formation of a zwitterion species of the carbamic acid ($MAEH^+CO_2^-$) through reaction 3. The spectral evidence, described before, of the protonation of MAE and the formation of the $CO_2^-$ group might imply the presence of $MAEH^+CO_2^-$ in the reaction system. The relative Raman intensities of the corresponding bands for liquid MAE saturated with $CO_2$ and aqueous solution of MAE saturated with $CO_2$ are, however, better explained by the formation of the two species $MAEH^+$ and $MAECO_2^-$ (Figures 6c and 7a). To examine the stability of $MAEH^+CO_2^-$, we have attempted the structural optimization of this species by ab initio calculations. The calculations showed that the structures of the $S^-G^-g^+$, $S^-G^+t$, and $G^+Tg^-$ conformers of $MAEH^+CO_2^-$ were actually dissociated into $CO_2$ and the $TG^-g^+$, $TG^+t$, and $G^+Tg^-$ conformers, respectively, of MAE. These results indicate that the zwitterion $MAEH^+CO_2^-$ should be essentially very unstable, similar to $NH_3^+CO_2^-$,[30,31] and is most probably a transition species even if it is formed through reaction 3.

The above discussions of the chemical species produced in the $CO_2$−MAE system have revealed that reaction 1 occurs in this system to give $MAECO_2^-$ and $MAEH^+$. The species $MAECO_2H$ and $MAEH^+CO_2^-$ expected through reactions 2 and 3 would be intermediate and transition species, respectively, even if they are formed.

A comparison of the Raman spectrum of liquid MAE saturated with $CO_2$ with that of liquid MAE saturated with hydrogen chloride, where the protonated species $MAEH^+$ is formed,[10] indicates that the bands at 533 and 835 $cm^{-1}$ are associated with $MAEH^+$ and the bands at 503, 606, 810, 860, and 949 $cm^{-1}$ are associated with $MAECO_2^-$. The bands of $MAECO_2^-$ are elucidated below on the basis of the normal vibrations of the lowest-energy conformers $S^-G^-g^+$, $S^-G^+g^-$, and $G^+Tg^-$, calculated by the HF/6-31G** method. The highest wavenumber of the skeletal deformation vibrations is 498 $cm^{-1}$ for $S^-G^-g^+$, 493 $cm^{-1}$ for $S^-G^+g^-$, and 421 $cm^{-1}$ for $G^+Tt$, the former two being in good agreement with the observed wavenumber 503 $cm^{-1}$. The calculated wavenumbers of the $CO_2$ deformation vibrations are 608 and 613 $cm^{-1}$ for $S^-G^-g^+$, 609 and 621 $cm^{-1}$ for $S^-G^+g^-$, and 603 and 639 $cm^{-1}$ for $G^+Tt$. The C−N stretching vibrations giving strong Raman intensities are calculated at 808 and 874 $cm^{-1}$ for $S^-G^-g^+$, 808 and 879 $cm^{-1}$ for $S^-G^+g^-$, and 848 and 987 $cm^{-1}$ for $G^+Tt$; the calculated results for the first two conformers correspond well with the observation of the strong Raman bands at 810 and 860 $cm^{-1}$. The vibration associated with the C−C stretching and $CH_2$ rocking modes is calculated at 931 $cm^{-1}$ for $S^-G^-g^+$ and 914 $cm^{-1}$ for $S^-G^+g^-$, in comparison with the observed wavenumber 949 $cm^{-1}$. These results demonstrate that the Raman bands of $MAECO_2^-$ are explained by the vibrations of the $S^-G^-g^+$ and $S^-G^+g^-$ conformers.

**TABLE 3: Observed and Calculated Vibrational Wavenumbers[a] ($cm^{-1}$) of $MAECO_2^-$ and $MAEH^+$**

| infrared[b] | Raman[b] | | | | | $MAECO_2^-$ ($S^-G^-g^+$) | | $MAEH^+$ ($TG^{\pm}t$) | |
|---|---|---|---|---|---|---|---|---|---|
| $CO_2$ liq[c] | $CO_2$ liq[c] | aq soln[d] | $CO_2$ aq soln[e] | HCl aq soln[f] | HCl liq[g] | HF/ 6-31G**[h,i] | B3LYP/ 6-31G*[h,j] | HF/ 6-31G**[h,i] | B3LYP/ 6-31G*[h,j] |
| 1173 w | 1174 m | 1170 mw[k] | 1171 m | 1162 br, mw | 1156 br, w | | | 1174 (4, 2) | 1166 (5) |
| 1151 w | | 1150 w[k] | | 1150 br, mw | | 1141 (8, 5) | 1140 (10) | | |
| 1113 vw | | 1112 m[k] | | | 1110 w | | | | |
| 1078 s | 1076 m | | 1081 s | 1078 ms | 1078 m | 1124 (81, 6) | 1108 (59) | 1120 (11, 3) | 1124 (11) |
| 1052 s | 1050 sh, s | | 1065 s[l] | 1065 sh, m | 1064 m | 1082 (32, 4) | 1076 (24) | 1098 (68, 5) | 1068 (59) |
| | | 1051 s[k] | | | | | | | |
| 1038 vs | 1038 s | | 1030 vs | 1029 s | 1036 m | 1045 (44, 5) | 1034 (53) | 1038 (7, 0.4) | 1040 (6) |
| | | 1022 s[k] | | | | | | | |
| 1009 sh, vw | 1009 w | | 1008 sh, s | 997 mw | 998 w | | | 992 (31, 7) | 995 (17) |
| | | 989 vw[k] | | | | | | | |
| | | 967 vw | 965 w | 962 mw | 965 w | | | 952 (20, 1) | 958 (18) |
| 949 w | 949 m | 950 w | 952 w | 943 vw | 948 w | 931 (82, 3) | 910 (84) | | |
| | | 896 br, w[k] | 911 vw | 905 m | 912 w | | | 894 (17, 5) | 897 (22) |
| 860 m | 860 s | 861 m | 859 s | | | 874 (11, 4) | 873 (10) | | |
| | | | | 840 s | | | | | |
| 831 vw | 835 m | 830 s[k] | 832 s | 824 s | 831 s | 840 (82, 0.6) | 824 (96) | 819 (13, 8) | 829 (12) |
| 813 s | 810 s | 821 sh, s | 820 sh, s | 799 mw | 809 sh, w | 808 (20, 11) | 798 (18) | 782 (4, 1) | 794 (3) |
| 786 vw | 786 sh, w | | | | | 741 (76, 0.3) | 781 (5) | | |
| 662 w | | | 675 w[m] | | | | | | |
| | | | 632 w[m] | | | | | | |
| | 613 sh, mw | | | | | 613 (7, 4) | 598 (10) | | |
| 610 ms | 606 mw | 607 w | 612 w | | | 608 (10, 2) | 593 (3) | | |
| 533 vw | 533 w | 536 mw[k] | 533 mw | 533 m | 536 w | | | 540 (14, 2) | 542 (14) |
| 503 w | 503 w | 509 w[k] | 509 sh, vw | 508 sh, vw | 511 sh, vw | 498 (2, 2) | 492 (0.7) | | |
| | | 459 vw[k] | | | | | | | |
| 418 mw | 418 mw | 422 m[k] | 421 sh, w | | 419 sh, w | 399 (11, 1) | 383 (8) | | |
| | | | 410 w | 407 w | 411 w | | | | |
| | 369 mw | 369 m[k] | 366 mw | 362 m | 369 m | 342 (9, 0.7) | 350 (12) | 365 (8, 1) | 375 (8) |
| | | 280 sh, vw[k] | | 283 sh, vw | 291 vw | 300 (2, 0.3) | 293 (3) | 318 (160, 3) | 314 (134) |
| | | | | | | | | 259 (11, 0.2) | 269 (10) |
| | | | | | | 220 (11, 0.1) | 249 (11) | 235 (12, 0.0) | 233 (19) |
| | | | | | | 179 (6, 0.3) | 187 (5) | 171 (18, 0.1) | 182 (14) |
| | | | | | | 133 (2, 0.4) | 135 (1) | | |
| | | | | | | 101 (0.4, 0.5) | 105 (0.4) | 94 (4, 0.0) | 99 (4) |
| | | | | | | 49 (1, 0.3) | 56 (0.8) | | |

[a] Wavenumbers above 1200 $cm^{-1}$ are not included in this table because they are insensitive to the conformation. [b] Approximate relative intensities: vs, very strong; s, strong; ms, medium strong; m, medium; mw, medium weak; w, weak; vw, very weak; sh, shoulder; br, broad. [c] Liquid MAE saturated with $CO_2$. [d] 30% aqueous solution of MAE in which $CO_2$ is slightly absorbed. [e] 30% aqueous solution of MAE saturated with $CO_2$. [f] Hydrochloric acid solution of MAE. [g] Liquid MAE saturated with hydrogen chloride. [h] For scale factors, see text. [i] Infrared intensities in km $mol^{-1}$ and Raman intensities in $Å^4$ $amu^{-1}$ are given in parentheses in this order. [j] Infrared intensities in km $mol^{-1}$ are given in parentheses. [k] Assigned to MAE. [l] Also assignable to carbonate ion ($CO_3^{2-}$). [m] Assigned to hydrogencarbonate ion ($HCO_3^-$).

Considering the calculated results of the conformational stabilities of $MAECO_2^-$ that the $S^-G^-g^+$ conformer is far more stable than others, we conclude that the conformer of $MAECO_2^-$ present in the $CO_2$−MAE system is most likely $S^-G^-g^+$, which is stabilized by strong intramolecular 1,6-OH···$O^-$ hydrogen bonding. This hydrogen bonding may well precede intermolecular interactions in the liquid state. The bands of $MAEH^+$, on the other hand, are interpreted on the basis of the calculated results shown in Figure 7 to be due to the $TG^{\pm}t$ conformer, which is stabilized by strong intramolecular 1,4-$NH^+$···O hydrogen bonding.

**$CO_2$−MAE−$H_2O$ System.** Figure 7 shows the Raman spectra of 30% aqueous solution of MAE saturated with $CO_2$ and hydrochloric acid solution of MAE, where $MAEH^+$ is formed. The calculated Raman spectra of the most stable three conformers of $MAEH^+$, $TG^{\pm}t$, $G^{\pm}G^{\pm}t$, and TTt, are also shown in this figure. The wavenumbers for these observed and calculated spectra are given in Table 3.

The Raman bands observed for an aqueous solution of MAE saturated with $CO_2$ (Figure 7a) correspond well to the observed bands for liquid MAE saturated with $CO_2$ (Figure 6c) except for their relative intensities and the observation of the three bands at 632, 675, and 1361 $cm^{-1}$ due to the hydrogencarbonate ion ($HCO_3^-$)[34] in the aqueous solution. This spectral finding indicates that the two chemical species $MAECO_2^-$ and $MAEH^+$ are formed in the $CO_2$−MAE−$H_2O$ system, and the conformations of these species are the same as those in the $CO_2$−MAE system. The spectrum of hydrochloric acid solution of MAE (Figure 7b), where only protonated MAE ($MAEH^+$) is expected, is close to the spectrum of liquid MAE saturated with hydrogen chloride (Figure 6a).

The Raman bands characteristic of $MAEH^+$ are observed at 533 and 824 $cm^{-1}$ in a hydrochloric acid solution of MAE. According to the HF/6-31G** calculations, the former band is assigned to the highest-wavenumber skeletal deformation vibration and the latter band is assigned to the C−N stretching vibration giving strong Raman intensity. The calculated wavenumbers for these vibrations are 540 and 819 $cm^{-1}$ for the $TG^{\pm}t$ conformer, 554 and 772 $cm^{-1}$ for the $G^{\pm}G^{\pm}t$ conformer, and 445 and 886 $cm^{-1}$ for the TTt conformer. These results clearly show that the observed bands at 533 and 824 $cm^{-1}$ are consistent only with the $TG^{\pm}t$ conformer of $MAEH^+$.

The above spectral interpretation confirms that MAE molecules in hydrochloric acid solution and in the liquid saturated with hydrogen chloride are protonated as $MAEH^+$, which assumes mostly the $TG^{\pm}t$ conformation stabilized by strong

intramolecular 1,4-$NH^+\cdots O$ hydrogen bonding rather than intermolecular hydrogen bonding. This is the same result as obtained for $DMAEH^+$.[9]

Reaction 1 in the $CO_2-MAE$ system implies that the same numbers of $MAECO_2^-$ and $MAEH^+$ molecules are produced through this reaction. The relative intensities of the Raman bands for $MAECO_2^-$ and $MAEH^+$ in liquid MAE saturated with $CO_2$ (Figures 6c) and in an aqueous solution of MAE saturated with $CO_2$ (Figure 7a) indicate that more $MAEH^+$ molecules are present than $MAECO_2^-$ molecules in the $CO_2-MAE-H_2O$ system. In Figure 7a, the bands at 509, 612, 820, 859, and 952 $cm^{-1}$ are associated with the $S^-G^-g^+$ conformer of $MAECO_2^-$ and the bands at 533 and 832 $cm^{-1}$ are associated with the $TG^{\pm}t$ conformer of $MAEH^+$, as interpreted before for liquid MAE saturated with $CO_2$. A previous NMR study of the $CO_2-MAE-H_2O$ system has shown that nearly the same amounts of $MAECO_2^-$ and $MAEH^+$ are formed in the initial stage of reaction, and after a half molar $CO_2$/MAE loading, the amount of $MAECO_2^-$ decreases with increasing amount of $MAEH^+$.[2]

On the basis of the present spectroscopic results complemented by the NMR results, we propose the following reactions for the $CO_2-MAE-H_2O$ system:

$$2CH_3NHCH_2CH_2OH\ (MAE) + CO_2 \rightleftharpoons CH_3N(CO_2^-)CH_2CH_2OH\ (MAECO_2^-) + CH_3NH_2^+CH_2CH_2OH\ (MAEH^+) \quad (4)$$

$$CH_3N(CO_2^-)CH_2CH_2OH\ (MAECO_2^-) + H_2O \rightleftharpoons CH_3NHCH_2CH_2OH\ (MAE) + HCO_3^- \quad (5)$$

$$CH_3NHCH_2CH_2OH\ (MAE) + CO_2 + H_2O \rightleftharpoons CH_3NH_2^+CH_2CH_2OH\ (MAEH^+) + HCO_3^- \quad (6)$$

Carbonate ion $CO_3^{2-}$ is also present in the $CO_2-MAE-H_2O$ system, and its amount depends on pH of the solution as expected from the dissociation constant of $HCO_3^-$. For a secondary amine MAE, reaction 4 occurs dominantly at the first stage and reactions 5 and 6 occur subsequently, while for a tertiary amine DMAE, only reaction 6 occurs.[9] The reaction mechanism of the $CO_2-amine-H_2O$ system is thus contrasted between the secondary amine (MAE) and the tertiary amine (DMAE).

The conformations of the chemical species in the $CO_2-MAE-H_2O$ system are summarized as follows: the main conformers present are $S^-G^-g^+$ for $MAECO_2^-$ and $TG^{\pm}t$ for $MAEH^+$. Intramolecular 1,6-$OH\cdots O^-$ hydrogen bonding in the $S^-G^-g^+$ conformer of $MAECO_2^-$ and intramolecular 1,4-$NH^+\cdots O$ hydrogen bonding in the $TG^{\pm}t$ conformer of $MAEH^+$ are strong enough to maintain their specific conformations even in the condensed phases such as in aqueous solution and in the liquid state. For MAE molecules in the condensed phases, on the other hand, intramolecular 1,4-$OH\cdots N$ hydrogen bonding in the $TG^+g^-$ and $G^-G^-g^+$ conformers is weaker than intermolecular $OH\cdots O$ or $OH\cdots N$ hydrogen bonding that stabilizes the $TG^-x$ conformers. Strong hydrogen bonding, in which ions are involved, has been found for $FH\cdots F^-$, $OH\cdots O^-$, and $OH^+\cdots O$.[35-37]

## Conclusions

The present vibrational spectroscopic and ab initio theoretical studies have shown that the chemical species produced in the reaction system of aqueous MAE solutions with dissolved $CO_2$ ($CO_2-MAE-H_2O$ system) are the carbamate anion ($MAECO_2^-$), the protonated cation ($MAEH^+$), hydrogencarbonate ion ($HCO_3^-$), and carbonate ion ($CO_3^{2-}$), while the species produced in the system of liquid MAE with dissolved $CO_2$ ($CO_2-MAE$ system) are $MAECO_2^-$ and $MAEH^+$. In the $CO_2-MAE-H_2O$ system, MAE (secondary amine) reacts with $CO_2$ to form $MAECO_2^-$ and $MAEH^+$, and $MAECO_2^-$ subsequently reacts with $H_2O$ and $CO_2$ to form $MAEH^+$ and $HCO_3^-$. This reaction mechanism is contrasted with the mechanism for 2-(*N*,*N*-dimethylamino)-ethanol (DMAE, tertiary amine), which reacts with $CO_2$ and $H_2O$ to form directly $DMAEH^+$ and $HCO_3^-$. In the liquid state and in aqueous solution, $MAECO_2^-$ molecules assume predominantly the $S^-G^-g^+$ conformation with the formation of strong intramolecular 1,6-$OH\cdots O^-$ hydrogen bonding, and $MAEH^+$ molecules assume predominantly the $TG^{\pm}t$ conformation with the formation of strong intramolecular 1,4-$NH^+\cdots O$ hydrogen bonding. MAE molecules in the condensed phases, on the other hand, assume several conformations such as $TG^-x$ ($x$ = t, $g^-$, and $g^+$), $TG^+g^-$, and $G^-G^-g^+$ as the result of the competition of intermolecular interactions such as $OH\cdots O$ or $OH\cdots N$ hydrogen bonding and intramolecular interactions such as the 1,4-$OH\cdots N$ hydrogen bonding. The interconversion, depending on pH or addition/removal of $CO_2$, of strong ionic hydrogen bonding such as $NH^+\cdots O$, $NH^+\cdots O^-$, and $OH\cdots O^-$ and nonionic hydrogen bonding such as $OH\cdots N$ and $OH\cdots O$ is clearly one of the important structural features in the $CO_2-amine-H_2O$ system and probably in biomolecular systems, where intramolecular and/or intermolecular interactions between nitrogen and oxygen atoms are involved.

**Acknowledgment.** We thank Dr. Toru Iwaki of Mitsubishi Heavy Industries, Ltd. and Dr. Taiichiro Suda of the Kansai Electric Power Co., Inc. for their helpful discussions.

## References and Notes

(1) Camacho, F.; Sánchez, S.; Pacheco, R. *Ind. Eng. Chem. Res.* **1997**, *36*, 4358−4364.
(2) Suda, T.; Iwaki, T.; Mimura, T. *Chem. Lett.* **1996**, 777−778.
(3) Xu, S.; Wang, Y.; Otto, F. D.; Mather, A. E. *Chem. Eng. Sci.* **1996**, *51*, 841−850.
(4) Saha, A. K.; Bandyopadhyay, S. S.; Biswas, A. K. *Chem. Eng. Sci.* **1995**, *50*, 3587−3598.
(5) Hagewiesche, D. P.; Ashour, S. S.; Al-Ghawas, H. A.; Sandall, O. C. *Chem. Eng. Sci.* **1995**, *50*, 1071−1079.
(6) Rinker, E. B.; Ashour, S. S.; Sandall, O. C. *Chem. Eng. Sci.* **1995**, *50*, 755−768.
(7) Andrés, J.; Moliner, V.; Krechl, J.; Silla, E. *J. Chem. Soc., Perkin Trans. 2* **1993**, 521−523.
(8) Benitez-Garcia, J.; Ruiz-Ibanez, G.; Al-Ghawas, H. A.; Sandall, O. C. *Chem. Eng. Sci.* **1991**, *46*, 2927−2931.
(9) Ohno, K.; Matsumoto, H.; Yoshida, H.; Matsuura, H.; Iwaki, T.; Suda, T. *J. Phys. Chem. A* **1998**, *102*, 8056−8062.
(10) Ohno, K.; Matsuura, H.; Iwaki, T.; Suda, T. *Chem. Lett.* **1998**, 531−532.
(11) Meredith, J. C.; Johnston, K. P.; Seminario, J. M.; Kazarian, S. G.; Eckert, C. A. *J. Phys. Chem.* **1996**, *100*, 10837−10848.
(12) Quinn, R.; Appleby, J. B.; Pez, G. P. *J. Am. Chem. Soc.* **1995**, *117*, 329−335.
(13) Hisatsune, I. C. *Can. J. Chem.* **1984**, *62*, 945−948.
(14) Curmi, P. M. G.; Cascio, D.; Sweet, R. M.; Eisenberg, D.; Schreuder, H. *J. Biol. Chem.* **1992**, *267*, 16980−16989.
(15) Lorimer, G. H. *Biochemistry* **1981**, *20*, 1236−1240.
(16) Scott, A. P.; Radom, L. *J. Phys. Chem.* **1996**, *100*, 16502−16513.
(17) Frisch, M. J.; Trucks, G. W.; Schlegel, H. B.; Gill, P. M. W.; Johnson, B. G.; Robb, M. A.; Cheeseman, J. R.; Keith, T.; Petersson, G. A.; Montgomery, J. A.; Raghavachari, K.; Al-Laham, M. A.; Zakrzewski, V. G.; Ortiz, J. V.; Foresman, J. B.; Cioslowski, J.; Stefanov, B. B.; Nanayakkara, A.; Challacombe, M.; Peng, C. Y.; Ayala, P. Y.; Chen, W.; Wong, M. W.; Andres, J. L.; Replogle, E. S.; Gomperts, R.; Martin, R. L.; Fox, D. J.; Binkley, J. S.; Defrees, D. J.; Baker, J.; Stewart, J. P.; Head-Gordon, M.; Gonzalez, C.; Pople, J. A. *GAUSSIAN 94*, revision D.3; Gaussian Inc.: Pittsburgh, PA, 1995.

(18) Yoshida, H.; Tanaka, T.; Matsuura, H. *Chem. Lett*. **1996**, 637−638.
(19) Yoshida, H.; Kaneko, I.; Matsuura, H.; Ogawa, Y.; Tasumi, M. *Chem. Phys. Lett*. **1992**, *196*, 601−606.
(20) Astrup, E. E. *Acta Chem. Scand., Ser. A* **1979**, *33*, 655−664.
(21) Yoshida, H.; Harada, T.; Ohno, K.; Matsuura, H. *Chem. Commun*. **1997**, 2213−2214.
(22) Masatoki, S.; Ohno, K.; Yoshida, H.; Matsuura, H. *J. Phys. Chem*. **1996**, *100*, 8487−8498.
(23) Räsänen, M.; Aspiala, A.; Homanen, L.; Murto, J. *J. Mol. Struct*. **1982**, *96*, 81−100.
(24) Frei, H.; Pimentel, G. C. *Annu. Rev. Phys. Chem*. **1985**, *36*, 491−524.
(25) Barnes, A. J. *J. Mol. Struct*. **1984**, *113*, 161−174.
(26) Ohno, K.; Yoshida, H.; Watanabe, H.; Fujita, T.; Matsuura, H. *J. Phys. Chem*. **1994**, *98*, 6924−6930.
(27) Barnes, A. J.; Hallam, H. E. *Trans. Faraday Soc*. **1970**, *66*, 1932−1940.
(28) van Thiel, M.; Becker, E. D.; Pimentel, G. C. *J. Chem. Phys*. **1957**, *27*, 95−99.
(29) Wright, H. B.; Moore, M. B. *J. Am. Chem. Soc*. **1948**, *70*, 3865−3866.
(30) Ramachandran, B. R.; Halpern, A. M.; Glendening, E. D. *J. Phys. Chem. A* **1998**, *102*, 3934−3941.
(31) Wen, N.; Brooker, M. H. *J. Phys. Chem*. **1995**, *99*, 359−368.
(32) Yoshida, Y.; Ishii, S.; Watanabe, M.; Yamashita, T. *Bull. Chem. Soc. Jpn*. **1989**, *62*, 1534−1538.
(33) Silverstein, R. M.; Bassler, G. C.; Morrill, T. C. *Spectrometric Identification of Organic Compounds*, 5th ed.; Wiley: New York, 1991.
(34) Palmer, D. A.; van Eldic, R. *Chem. Rev*. **1983**, *83*, 651−731.
(35) Huggins, M. L. *Angew. Chem., Int. Ed. Engl*. **1971**, *10*, 147−152.
(36) Joesten, M. D. *J. Chem. Educ*. **1982**, *59*, 362−366.
(37) Jeffrey, G. A.; Saenger, W. *Hydrogen Bonding in Biological Structures*, 2nd ed.; Springer: Berlin, 1994.